COMPARING THE CYSTALLOGRAPHIC STRUCTURES OF THE HOWARDITE, EUCRITE AND DIOGENITE (HED) METEORITES. L.V. Forman[1], L. Daly[2,1], T. J. Barrett[3], [1]Space Science and Technology Centre, School of Earth and Planetary Science, Curtin University, Bentley, 6102, Australia. (lucy.forman@curtin.edu.au), [2]School of Geographical and Earth Sciences, University of Glasgow, Glasgow, G12 8QQ, UK. [3]Open University, Milton Keynes, MK7 6AA, UK,

Introduction: The Howardite, Eucrite, Diogenite (HED) meteorites are a group of achondrite meteorites that likely originate from the same parent body (e.g. [1, 2]), which is believed to be 4 Vesta [3]. As HED meteorites are some of the oldest achondrites in our collections [4], they can provide valuable insights into processes occurring on small bodies early in the Solar System.

To provide further constraints of the geological history of the HED parent body, we are undertaking a systematic cryatallographic analysis of a suite of HED meteorites by using electron backscatter diffraction (EBSD) analyses. Preliminary work has focused on the meteorties Allan Hills (ALH) 88135, a howardite polymict breccia, and Camel Donga, a eucrite monomict breccia.

Method: Thin sections of each sample were polished using 1 µm and 0.3 µm alluminium sphere suspension fluid for 15 minutes each, and a colloidal silica NaOH suspension for 4 hours. The sections were left uncoated to permit analysis at low vaccum. EBSD analyses were conducted on the samples using the Zeiss Sigma variable pressure field emission scanning electron microscope (VP-FE-SEM) at the Imaging Spectroscopy and Analysis Centre, at the University of Glasgow. Samples were tilted to 70°, which is typical for EBSD analyses. The samples were analysed at 20 kV with a low current <4 nA to avoid volatile element mobility in minerals such as apatite [5,6] and data were collected at a step size of 3.5 µm. Small areas of 1.1 mm^2 and 0.3 mm^2 were imaged from Camel Donga (Figure 1) and ALH 88135 (Figure 2) respectively. The data were collected using the Aztec software package and processed using the Channel 5 software package from Oxford Instruments. The data were cleaned for artifacts using a single wildspike correction and a eight and seven point iterative nearest neighbor zero solution. Deformation microstructures within the pyroxenes were evaluated by plotting crystal rotation axes for both ortho- and clinopyroxenes (Figure 3). Grains were defined using the 'grain detect' algorithm using a 10 degree misorientation threshold for adjacent pixels.

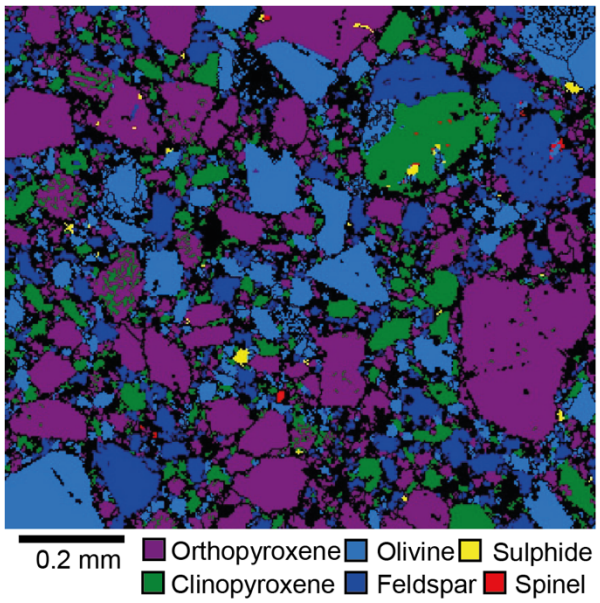

Figure 2. An EBSD phase map of ALH 88135. The colours reveal the distribution of each mineral phase within this region.

Results: *Mineralogy:* The EBSD data reveal

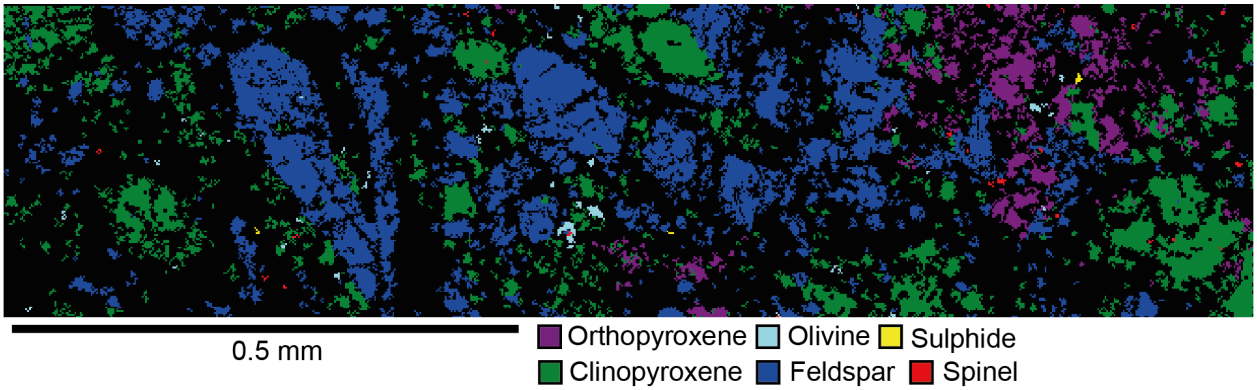

Figure 1. An EBSD phase map of Camel Donga. The colours reveal the distribution of each mineral phase within this region.

Camel donga is comprised of clinopyroxene (40%) and feldspar (55%) with minor amounts of olivine (~3%), spinel (~1%) and sulphides (~1%) (Figure 1). The feldspar and pyroxene are intergrown. ALH 88135 is comprised of both clinopyroxene (30%) and orthopyroxene (26%), with felspar (25%) and minor spinel (0.5%) and sulphide (1.5%) (Figure 2). ALH 88135 also contains a higher abundance of olivine (17%) relative to Camel Donga (~3%) (Figure 1, 2).

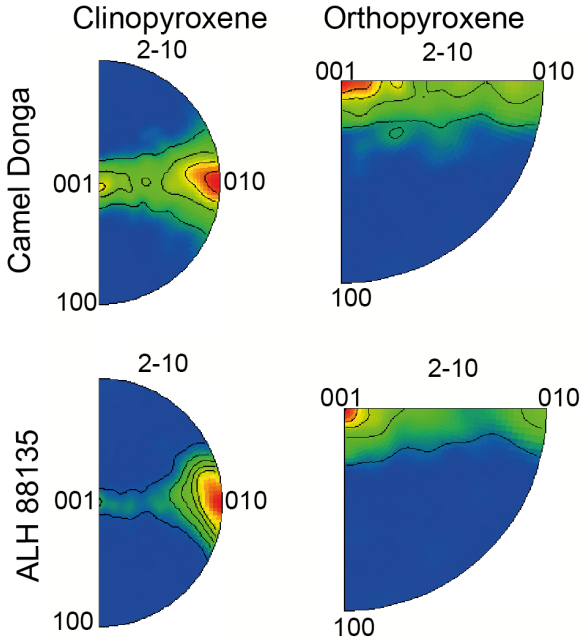

Figure 3. The prinicipal rotation axes of clinopyroxene and orthopyroxene in camel Donga and ALH 88135.

In some regions of ALH 88135, clinopyroxene is exsolving from the orthopyroxene as twins (Figure 2).

Deformation microstructures: There are subtle differences in the active slip systems between ALH 88135 and Camel Donga. ALH 88135 is dominated by slip systems rotating around <010> within the clinopyroxene, and <001> in the orthopyroxene. Conversely, the clinopyroxene and orthopyroxene in Camel Donga are defined by a spread of rotation axis between <001> and <010> (Figure 3). In both samples the two dominant slip systems present in the orthopyroxene are (100)[010] and (100)[001].

Discussion: The mineralogy of these regions are broadly consistent with the published literature (e.g. [7, 8]). The olivine content of Camel Donga, however, is somewhat higher than anticipated for Eucrites [7]. The modal mineralogy of ALH 88135 has not been previously determined so this data represents the first estimate of this meteorites modal mineralogy.

The differences between the deformation microstructures in Howardites and Eucrites observed here are intriguing. Typical shock indicators such as mechanical twinning in pyroxene [9] are not observed in either sample and both samples have very low amounts of internal strain within the grains. As these samples are breccias, the lack of evidence for shock deformation may be due to recovery of these microstructures during post-shock, high temperature annealing [10]. This is somewhat supported by the prevelance of the (100)[001] slip system in orthopyroxene in both samples, which dominates at temperatures above 1000°C [11]. However, (100)[001] slip is also the most commonly found slip system in terrestrial orthopyroxenes [11] and furthermore, we cannot rule out a magmatic origin for these textures that would also provide sufficiently high temperatures to activate the (100)[001] slip system.

The occurrence of the (100)[010] slip system here is unusual as it has not been reported previously in naturally deformed terrestrial or extraterrestrial rocks [11]. (100)[010] slip has only been reported in experiemtnatlly deformed orthopyroxenes when the [001] is perpendicular to compression direction [11]. If this is the case here, then it will be possible to derive the direction of compression.

These preliminary results are intriguing and warrant further exploration. We are currently undertaking large area mapping of the whole thin sections using the Symmetry EBSD detector at Curtin University. The results of these large area maps will be presented and discussed at the meeting.

References: [1] Scott E. R. D., et al., (2009) *Geochimica et Cosmochimica Acta* 73, 19, 5835-5853. [2] Greenwood R. C., et al., (2014) *Earth and Planetary Science Letters* 390, 165-174. [3] McSween H. Y. et al. (2013) *Meteoritics and Planetary Sciences* 48, 11, 2090-2104. [4] Misawa K., et al., (2005) *Geochimica et Cosmochimica Acta,* 69, 24, 5847-5861. [5] Goldoff B., et al. (2012) *Amierican Mineralogist* 97, 1103-1105. [6] Stock M. J., et al., (2015) *American Mineralogist* 100, 281-293. [7] Delaney J. S., et al., (1984) *Journal of Geophysical Research:Solid Earth* 89, S01, C251-C288. [8] Bowman L. E. et al., (1997) *Meteoritics and Planetary Sciences* 32(6), 869-875. [9] Stöffler D. and Kiel K., (1991), *Geochimica et Cosmochimica Acta*, 55, 3845-3867 [10] Song R., et al., (2005) *Acta. Materiala*, 53, 845-858 [11] Raleigh C.B., et al., (1971), *Journal of Geophysical Research*, 76, 4011-4022.

Acknowledgements: The authors would like to thank the technical expertise and electron microscopy facilities at the Imaging Spectroscopy and Analysis Centre, at the University of Glasgow. We would also like to thank The Open University for the loan of the samples.